Journal of Structural Biology 169 (2010) 200–208

Contents lists available at ScienceDirect

Journal of Structural Biology

journal homepage: www.elsevier.com/locate/yjsbi

Structure of dihydropyrimidinase from *Sinorhizobium meliloti* CECT4114: New features in an amidohydrolase family member

Sergio Martínez-Rodríguez [a,*,1], Ana Isabel Martínez-Gómez [a], Josefa María Clemente-Jiménez [a], Felipe Rodríguez-Vico [a], Juan Ma García-Ruíz [b], Francisco Javier Las Heras-Vázquez [a], Jose Antonio Gavira [b,*,1]

[a] Dpto. Química Física, Bioquímica y Química Inorgánica, Universidad de Almería, Almería, Spain
[b] Laboratorio de Estudios Cristalográficos. IACT, CSIC-Universidad de Granada, Granada, Spain

ARTICLE INFO

Article history:
Received 18 June 2009
Received in revised form 1 October 2009
Accepted 24 October 2009
Available online 4 November 2009

Keywords:
Dihydropyrimidinase
Hydantoinase
Hydantoinase process
Amino acid production
Amidohydrolase superfamily

ABSTRACT

The recombinant dihydropyrimidinase from *Sinorhizobium meliloti* CECT4114 (SmelDhp) has been characterised and its crystal structure elucidated at 1.85 Å. The global architecture of the protein is reminiscent of that of the amidohydrolase superfamily, consisting of two domains; an $(\alpha/\beta)_8$ TIM-like barrel domain, where the catalytic centre is located, and a smaller β-sheet sandwich domain of unknown function. The c-terminal tails of each subunit extend toward another monomer in a swapping-like manner, creating a hydrogen bond network which suggests its implication in protein oligomerisation. Mutational and structural evidence suggest the involvement of a conserved tyrosine in the reaction mechanism of the enzyme. SmelDhp presents both hydantoinase and dihydropyrimidinase activities, with higher affinity for the natural six-membered ring substrates. For the five-membered ring substrates, affinity was greater for those with aliphatic and apolar groups in the 5th carbon atom, with the highest rates of hydrolysis for D-5-methyl and D-5-ethyl hydantoin (k_{cat}/K_m = 2736 ± 380 and 944 ± 52 M^{-1} s^{-1}, respectively). The optimal conditions for the enzyme activity were found to be 60 °C of temperature at pH 8.0. SmelDhp retains 95% of its activity after 6-hour preincubation at 60 °C. This is the first dihydropyrimidinase used for the hydrolytic opening of non-natural 6-monosubstituted dihydrouracils, which may be exploited for the production of β-amino acids.

1. Introduction

Dihydropyrimidinases (EC 3.5.2.2) are involved in the reductive pathway of pyrimidine degradation, catalysing the hydrolysis of 5,6-dihydrouracil and 5,6-dihydrothymine to the corresponding *N*-carbamoyl-β-amino acids. In humans, enzymes of the pyrimidine degradation pathway are responsible for degradation of the widely used cytotoxic chemotherapy drug 5-fluorouracil (5FU) (van Kuilenburg, 2004). In particular, patients with dihydropyrimidinase deficiency, an autosomal recessive disease characterised by dihydrothymine–dihydrouraciluria in homozygous deficient patients (van Kuilenburg et al., 2007), are prone to the development of severe 5FU-associated toxicity (Sumi et al., 1998; van Kuilenburg et al., 2003). However, dihydropyrimidinases have been more commonly known as hydantoinases, as this enzyme can be used in the production of optically pure amino acids starting from racemic mixtures of 5-monosubstituted hydantoins using the so-called "hydantoinase process", together with an enantiospecific carbamoylase and a hydantoin racemase (Martínez-Rodríguez et al., 2002; Martínez-Gómez et al., 2007). Although this process has been used industrially since the 1970s (Clemente-Jiménez et al., 2008), the ever increasing demand for side-chained D-amino acids has maintained the interest in this industrial process, even more so since the use of hydantoin racemase allows the total conversion of racemic hydantoins when chemical racemisation is not favoured (Las Heras-Vázquez et al., 2003; Martínez-Rodríguez et al., 2004a,b). Thus, the isolation of new hydantoinases/dihydropyrimidinases with different substrate specificities, improved activity, enantioselectivity or higher stability continues to be of great industrial interest.

This work presents a dihydropyrimidinase able to hydrolyse non-natural 5- and 6-monosubstituted dihydrouracils, which may be used for enzymatic production of β-amino acids. It also presents the first structural evidence of the involvement of a con-

* Corresponding authors. Addresses: Dpto. Química Física, Bioquímica y Química Inorgánica, Universidad de Almería, Edificio CITE I, Carretera de Sacramento s/n, 04120 La Cañada de San Urbano, Almería, Spain. Fax: +34 950 015615 (S. Martínez-Rodríguez); Laboratorio de Estudios Cristalográficos, Edf. López Neira, P.T. Ciencias de la Salud, Avenida del Conocimiento, s/n, 18100 Armilla, Granada, Spain. Fax: +34 958 181632 (J.A. Gavira).
E-mail addresses: srodrig@ual.es (S. Martínez-Rodríguez), jgavira@ugr.es (J.A. Gavira).
[1] Both authors contributed equally to this work and should be considered joint first authors.

1047-8477/$ - see front matter © 2009 Elsevier Inc. All rights reserved.
doi:10.1016/j.jsb.2009.10.013

Table 1
Data collection and refinement statistics of SmelDhp. Statistical values for the highest resolution shell (1.90–1.85 Å) are given in parentheses.

Data collection			
Wavelength (Å)	1.54	Resolution (Å)	39.9–1.85
Temperature (K)	100 K	Number of observed reflections	445,300
Space group	*C*222(1)	Redundancy	3.47 (1.83)
a, *b*, *c* (Å)	124.9, 126.3, 196.1	Completeness (%)	98.4 (89.1)
Matthews coefficient ($Å^3$ Da^{-1})	3.6	R_{MERGE}[a] (%)	6.2 (31.1)
Monomers per asymmetric unit	2	Average I/σ (I)	13.0 (3.1)
Refinement			
R value (%)	14.8 (20.3)	Average *B* factor ($Å^2$)	14.00
R_{free} value (%)	17.6 (26.0)	RMSD bond length (Å)	0.028
Number of reflections in working set	129,519	RMSD bond angles (°)	1.644
Number of reflections in test set	6524	Number of solvent molecules	1138
Number of heteroatom	4 Zn^{2+}	4 Glycerol	2 Acetate
Ramachandran plot			
Most favored regions (%)	91.5	Gener. allowed regions (%)	0.4
Allowed regions (%)	8.1	Disallowed regions (%)	0.0

[a] $R_{sym} = \sum_h\sum_i|(I_i(h)) - \langle I(h)\rangle|/\sum_h\sum_i I_i(h)$, where $I_i(h)$ is the ith measurement of reflection h, and $\langle I(h)\rangle$ is the weighted mean of all measurements of h.

served c-terminal tail of dihydropyrimidinases in protein dimerisation, and together with mutational studies it puts forward an important role of Tyr152 in the activity of the enzyme.

2. Material and methods

2.1. Mutation of SmelDhp Tyr152 and Arg476

Mutagenesis was performed using QuikChange II Site-directed mutagenesis kit from Stratagene following the manufacturer's protocol. For the mutations, the C-terminal His-tagged expression plasmid pSER38 harbouring the wild-type *SmelDhp* gene was used as template (Martínez-Rodríguez et al., 2006). Mutations were confirmed by using the dye dideoxy nucleotide sequencing method in an ABI 377 DNA Sequencer (Applied Biosytems).

2.2. Purification, crystallisation and data collection of SmelDhp

Procedures for the purification, crystallisation and data collection of Smeldhp are described in detail elsewhere (Martínez-Rodríguez et al., 2006). Briefly, the recombinant protein was overproduced including a His_6 tag and purified using cobalt affinity chromatography. SmelDhp activity required the presence of divalent metal ions such as Zn^{2+}. In order to obtain the holoenzyme, 20–50 μM of the purified enzyme was treated for 1 h at 4 °C with 0.5 mM $ZnCl_2$. This holoenzyme form of SmelDhp was used in all the experiments, except where otherwise indicated. Y152A and Arg476A smelDhp mutants were purified following the same protocol, next Gel Filtration experiments were carried out on a Superdex-200 column to evaluate a change in the oligomerisation of the enzymes.

Conditions leading to the production of well diffracting crystals of the wild-type enzyme were determined by the hanging drop method, and optimised using the counter-diffusion capillary technique (Martínez-Rodríguez et al., 2006). Data were collected from a single crystal on a BRUKER AXS MICROSTAR Proteum and processed using the PROTEUM software suite (Bruker AXS Inc.).

2.3. Structure determination and refinement

SWISS-MODEL server was used to calculate the initial model, using ProModII for modelling and GROMOS96 for energy minimisation (Schwede et al., 2000). Coordinates 1YNY (Radha Kishan et al., 2005), 1KCX (Deo et al., 2004) and 1K1D (Cheon et al., 2002) were used together with the SmelDhp sequence as input file. REFMAC5 (Murshudov et al., 1997) from the CCP4 software suite (Collaborative Computational Project, Number 4, 1994) was used to refine the structure keeping a 5% of the total reflections to calculate R_{free}. Coot (Emsley and Cowtan, 2004) was used for visualisation and manual rebuiliding of side chains and waters. Subsequently, water molecules were fitted manually by selecting densities from $2F_o - F_c$ maps, with corresponding positive peaks in $F_o - F_c$ maps, so that the molecules made hydrogen bonding contact with protein atoms or other water molecules. Heteroatoms (Zn^{2+}, acetate and glycerol) were added to the model and refined to *R* and R_{free} values of 19.2% and 21.6%, respectively. Further refinement included the definition of 20 TLS groups per amino acid chain (Winn et al., 2001). Refinement was stopped when no further water could be found meeting these premises, with final *R*-factor and R_{free} of 14.8% and 17.6%, respectively. After refinement the quality of the model was checked using MolProbity (Lovell et al., 2003) and previous deposition with PROCHECK (Laskowski et al., 1993) and WHAT_CHECK (Hooft et al., 1996). Refinement parameters and statistics of the final model of SmelDhp are summarised in Table 1. Coordinates and structure factors have been deposited at the RCSB PDB with entry code 3DC8.

Table 2
Relative activity of SmelDhp after preincubation with different metal ions and other chemical reagents at room temperature for 45 min. The experiments were conducted at pH 8, with 2 mM of reagent concentration, except for EDTA, HQSA, DTT and β-mercaptoethanol, in which the concentration was 10 mM.

Compound	Relative activity (%)
Non-treated	100 ± 5
$CuCl_2$	150 ± 2
$FeCl_2$	106 ± 1
NaCl	103 ± 2
$ZnCl_2$	432 ± 9
$MnCl_2$	407 ± 7
$CoCl_2$	331 ± 15
$HgCl_2$	0 ± 0
KCl	95 ± 7
$CaCl_2$	98 ± 7
$NiCl_2$	346 ± 7
$MgCl_2$	121 ± 8
$Pb(AcO)_2$	108 ± 5
$FeCl_3$	99 ± 9
EDTA	90 ± 0
HQSA	78 ± 5
DTT	111 ± 1
β-Mercaptoethanol	106 ± 15
DTNB	108 ± 5
Iodoacetamide	100 ± 3

Table 3
Kinetic parameters of SmelDhp toward different substrates. "Concentration" row indicates the highest concentration of each substrate used.

Substrate	K_m (mM)	k_{cat} (s^{-1})	k_{cat}/K_m (M^{-1} s^{-1})	Concentration (mM)	Mobile phase[b]	λ (nm)
Hydantoin	125 ± 17	12 ± 1	96 ± 13	200	100%C	
D-5-Methylhydantoin	72 ± 10	197 ± 12	2736 ± 380	200	95%A:5%B	200
D-5-Ethylhydantoin	18 ± 1	17 ± 0	944 ± 52	200	95%A:5%B	200
D-5-Propylhydantoin	26 ± 6	6 ± 0	231 ± 53	100	90%A:10%B	205
D-5-Butylhydantoin	14 ± 2	3 ± 0	214 ± 31	50	70%A:30%B	205
D-5-Methyl-thio-ethylhydantoin	66 ± 7	18 ± 1	273 ± 29	200	80%A:20%B	210
D-5-*iso*-Propylhydantoin	44 ± 3	5 ± 0	114 ± 8	160	90%A:10%B	205
D-5-*iso*-Butylhydantoin	10 ± 2	2 ± 0	200 ± 40	15	80%A:20%B	205
D,L-5-*iso*-Propylhydantoin	87 ± 10	5 ± 0	57 ± 7	160	90%A:10%B	205
D,L-5-*para*-Hydroxy-phenylhydantoin	20 ± 2	1 ± 0	50 ± 5	25	95%A:5%B	223
D,L-5-Phenylhydantoin	ND[a]			15	80%A:20%B	205
D-5-Benzylhydantoin	5 ± 1	2 ± 0	400 ± 80	15	70%A:30%B	210
D,L-5-Methyl-thio-ethylhydantoin	140 ± 34	12 ± 2	86 ± 21	200	80%A:20%B	210
Dihydrouracil	3 ± 0	2 ± 0	667 ± 0	60	100%C	200
D,L-5-Methyldihydrouracil	1 ± 0	1 ± 0	1000 ± 0	120	95%A:5%B	200
D,L-6-Methyldihydrouracil	111 ± 13	8 ± 0	72 ± 8	160	95%A:5%B	200
D,L-6-iso-Propyldihydrouracil	81 ± 3	1 ± 0	12 ± 0	120	85%A:15%B	200
D,L-6-Propyldihydrouracil	ND[a]			10	75%A:25%B	200
D,L-6-iso-Butyldihydrouracil	ND[a]			10	85%A:15%B	200

[a] The enzyme showed activity toward these substrates, but binding parameters could not be determined due to low solubility of the compounds.
[b] A = H_3PO_4 20 mM pH 3.2; B, methanol; C, NaH_2PO_4 20 mM pH 4.5.

2.4. Analysis of SmelDhp structure

DALI server (Holm et al., 2008) was used to search for similar folding to that presented by SmelDhp structure. PISA and PDBsum servers (Krissinel and Henrick, 2007; Laskowski et al., 2005) were used to analyse interfaces of SmelDhp. Pymol was used for graph generation (Delano, 2002).

2.5. Enzyme assay and protein characterisation

The monosubstituted hydantoins and dihydrouracils, and the corresponding *N*-carbamoyl-α or β-amino acids used in this work, were synthesised according to the potassium cyanate method for the carbamoylation and cyclation of amino acids, described elsewhere (Ware, 1950; Martínez-Rodríguez et al., 2007). Standard enzymatic reaction was carried out with SmelDhp (0.5–2.5 μM), together with D-5-methyl-thio-ethyl-hydantoin (D-MTEH) (100 mM) as substrate, dissolved in 200 mM sodium phosphate buffer (pH 8.0) in 200 μl reaction volume. The reaction mixture was incubated at 40 °C for 20 min and stopped by addition of four times the reaction volume of 1% H_3PO_4. After centrifugation, the supernatant was analysed by high performance liquid chromatography (Breeze HPLC System, Waters Cromatografia S.A., Barcelona, Spain) equipped with a LUNA C18(2) column (4.6 × 250 mm, 5 μm particle size, Phenomenex) to detect D-MTEH and *N*-carbamoyl-D-methionine. SmelDhp Y152A activity was measured using the standard activity assay described above, but using dihydrouracil instead D-MTEH as substrate. The same method was used to determine optimum temperature and pH by incubating the reaction mixture at 10–80 °C and/or at pH 5.5–6.5 (200 mM sodium cacodylate), pH 6.5–8.0 (200 mM sodium phosphate), pH 7.5–8.5 (200 mM Tris–HCl) and pH 8.5–10.5 (100 mM Borate HCl or NaOH). Thermal stability of the enzyme was determined with the holoenzyme, after 30-min preincubation at different temperatures from 20 to 80 °C, in 200 mM sodium phosphate buffer pH 8.0, followed by the standard activity assay. To analyse the effect of different compounds on the enzyme activity, samples of non-Zn-treated purified SmelDhp (3 μM) were incubated with them in 200 mM sodium phosphate buffer pH 8.0 (final volume 100 μl) at room temperature for 45 min (Table 2), followed by the standard enzyme assay. Temperature studies were completed by analyzing the ability of the chelating agents EDTA and HQSA (10 mM) to retrieve the cation from the catalytic site of the holoenzyme in the range of temperature 20–60 °C.

Substrate specificity and kinetic studies were performed with each different 5-monosubstituted hydantoin, 5- or 6-monosubstituted dihydrouracil dissolved in 200 mM sodium phosphate buffer (pH 8.0) together with the holoenzyme (0.5–2.5 μM). Reactions were carried out at 40 °C and stopped by addition of 1% H_3PO_4 at different times. The detection of the different substrates and their corresponding *N*-carbamoyl-α or β-amino acids was carried out with the HPLC system described above. The wavelengths and mobile phase used for each substrate are summarised in Table 3. The k_{cat} was defined as the mmol of *N*-carbamoyl-α or β-amino acid per second and mmol of enzyme at 40 °C.

3. Results and discussion

3.1. Characterisation and substrate specificity of SmelDhp

Maximum enzymatic activity proved to be at pH 8.0 and 60 °C (Supplementary Figures S1 and S2). SmelDhp enzyme maintained 95% of its activity when it was preincubated for 6 h at 60 °C, whereas it only retained 25% when preincubated for 30 min at 70 °C. Relative activity was greatly enhanced in the presence of Zn^{2+}, Mn^{2+}, Ni^{2+}, Co^{2+}, whereas Hg^{2+} caused total inhibition. EDTA and HQSA caused only 10% and 23% inactivation, respectively, when the preincubation was carried out at room temperature (Table 2). Retrieval of metal in SmelDhp required the presence of HQSA (rather than EDTA) and heating up to 60 °C (T_m of the protein was shown to be 63–65 °C in a previous work; Martínez-Rodríguez et al., 2009).

SmelDhp presents both hydantoinase and dihydropyrimidinase activity (Table 3), being enantioselective for the D-isomer of monosubstituted 5-hydantoins. Activity with substrate analogues such as allantoin, 5,5-dimethylhydantoin, 5-benzyl,5-methyl-hydantoin, succinimide, rodamine or tiazoledione was not detected under the conditions assayed (data not shown). Kinetic parameters were obtained from hyperbolic saturation curves by least-squares fit of the data to the Michaelis–Menton equation (Table 3). The

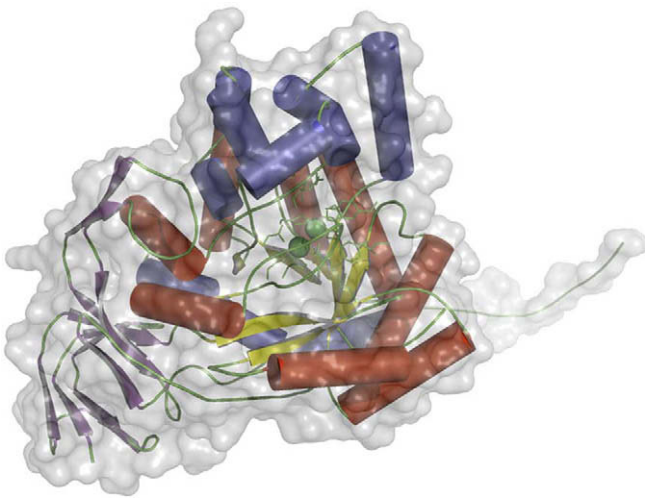

Fig. 1. Diagram illustrating the domain architecture of SmelDhp, showing the β-sandwich domain (purple), the alpha–beta barrel (red and yellow) and the additional alpha helices (dark blue) found inserted in the alpha–beta barrel. The catalytic site is shown as green sticks, with the two Zn ions presented as green spheres. (For interpretation of the references to color in this figure legend, the reader is referred to the web version of this paper.)

highest affinity with the studied substrates was found with 5-methyldihydrouracil and dihydrouracil, the two natural substrates of this enzyme, followed by D-5-benzyl-hydantoin.

3.2. Overall structure of SmelDhp

Two structurally identical polypeptide chains are present in the asymmetric unit, with a RMSD of 0.25 Å for 475 common alpha-carbon atomic pairs, and 0.46 Å for all common atoms (3628). Chains A and B comprise 483 and 475 residues, respectively, out of 490 (including the His_6 tag). Pro96 could not be fitted into the electronic density for any of the chains. Chain B lacks Gly478-His490, although Chain A contains up to His485, the first residue belonging to the His_6 tag. Each chain has two Zn^{2+} atoms at the hydrolytic active centre and several other heteroatoms such as acetate ion and glycerol coming from the crystallisation and cryoprotectant solutions (Table 1). The architecture of SmelDhp is reminiscent of the amidohydrolase superfamily (Seibert and Raushel, 2005), presenting two domains (Fig. 1). The larger domain of this enzyme presents a distorted $(\alpha/\beta)_8$ TIM barrel, consisting of an inner ring of eight parallel β-strands[2] whose length decreases from the beginning to the end, wrapped by an outer wheel comprised of eight α-helices. This domain differs from a canonical TIM-barrel fold in that additional α-helices of different lengths appear intercalated in the barrel, partially covering its upper part (Fig. 1, dark blue).

The smaller domain is formed by 12 β-strands, located at the N- and C-termini, laterally attached in the lower part to the TIM barrel via two linkers formed by Pro50–Gly51 and the region Tyr376–Asp387. This β-sandwich domain has been identified in other amidohydrolase-related enzymes, such as allantoinase (PDB ID. 3E74; Kim et al., 2009), dihydroorotase (PDB ID. 1XRF; Martin et al., 2005), cytosine deaminase (PDB ID. 1K6W; Ireton et al., 2002), D-aminoacylase (PDB ID. 1M7J; Liaw et al., 2003), iso-aspartyl dipeptidase (PDB ID. 1PO9; Jozic et al., 2003), *N*-acetylglucosamine-6-phosphate deacetylase (PDB ID. 1UN7; Vincent et al., 2004), imidazalonepropionase (PDB ID. 2BB0; Yu et al., 2006), and enamidase (PDB ID. 2VUM, Kress et al., 2008). It has been subjected to SCOP classification, constituting an independent fold and a SCOP superfamily (composite domain of metallo-dependent hydrolases, SCOP 51337 and 51338), and has been suggested to have a structural role for several members of the amidohydrolase family (Ireton et al., 2002; Jozic et al., 2003; Liaw et al., 2003). In hydantoinases/dihydropyrimidinases, this domain has also been proposed to have a structural role or to be involved in a higher degree of oligomerisation, as it forms an eight-stranded extended sheet by the combination of two four-stranded β-sheets of two adjacent monomers (Cheon et al., 2002; Radha Kishan et al., 2005; Xu et al., 2003; Abendroth et al., 2002a,b; Lohkamp et al., 2006). This extended β-sheet is not observed, however, in SmelDhp, nor was it in dihydropyrimidinase from *Dictyostelium discoideum* (^{Dd}DHPase, Lohkamp et al., 2006), or other homologue structures (Deo et al., 2004; Martin et al., 2005; Kress et al., 2008). Moreover, it is important to highlight the proposed regulatory role of two of the β-strands of the β-sandwich domain in the homologue collapsing response mediator protein (CRMP, Deo et al., 2004). More evidence is therefore needed to obtain a clear conclusion about the real role of this domain, which may not be limited to oligomerisation.

3.3. Oligomerisation interfaces in SmelDhp

Hydantoinases/dihydropyrimidinases in solution have commonly been described as homodimers (Xu and West, 1994; Lee et al., 1995; Xu et al., 2003) or homotetramers (Abendroth et al., 2002b; Cheon et al., 2002; Lohkamp et al., 2006). SmelDhp biological unit was shown to be a homotetramer by hydrodynamic and spectroscopic techniques (Martínez-Rodríguez et al., 2006; Martínez-Rodríguez et al., 2009). Inspection of the X-ray structure suggests that this homotetramer is formed by a dimer of dimers (Fig. 2A and B), in which each dimer consists of one of the subunits in the asymmetric unit and a twofold axis symmetry-generated monomer (Fig. 2A). In the dimeric arrangement, two principal contact interfaces can be distinguished, in which 45 and 42 residues participate from chains A and D, respectively (chain D lacks residues 478–484 from the tail). Twenty-six direct hydrogen bonds plus 270 van der Waals contacts are observed, with a covered area of 2095 and 2062 Å^2, respectively. The first and largest interface area is covered by coiled coil (α7A–α7D) and helix–helix interactions (α4A–α5D and α4D–α5A), where interacting residues D160–N183 and E216–R220 are completely conserved among the hydantoinase structures known to date (Fig. 2C), suggesting an important role in dimer formation. The second interface would be formed by the c-terminal tails (residues 472–485) of both subunits, which hook the counterpart monomer by forming several reciprocal hydrogen bonds and van der Wals contacts in a swap domain-like manner (Fig. 2A).

On the other hand, the homotetramerisation of SmelDhp occurs via oligomerisation of A–D and B–C dimers (Fig. 2B). The A–B interface comprises 12 close-range interactions (<3 Å) and 129 non-bonded contacts, with a covered area of 1213 and 1206 Å^2 for each monomer. Residues involved in oligomerisation appear principally in alpha helices and the loops continuing these helices. Both hydrophilic and hydrophobic interactions are involved in dimeric and tetrameric interface contacts, although the tetrameric assembly allows more non-polar amino acids to be buried than primary dimerisation. A PISA analysis of SmelDhp interfaces, predicts that both homotetramer and homodimer are stable in solution, with an ASA of 58,360 Å^2 and 31,530 Å^2, and a buried area of 12,960 Å^2 and 4140 Å^2, respectively. However, chemical and thermal denaturation of SmelDhp occurs directly from the tetramer to the monomer (Martínez-Rodríguez et al., 2009), and therefore

[2] The last β-strand would be formed by the segment Val309–Ala311, although it does not appear annotated in the PDB. Its appearance depends on which software is used for secondary structure prediction.

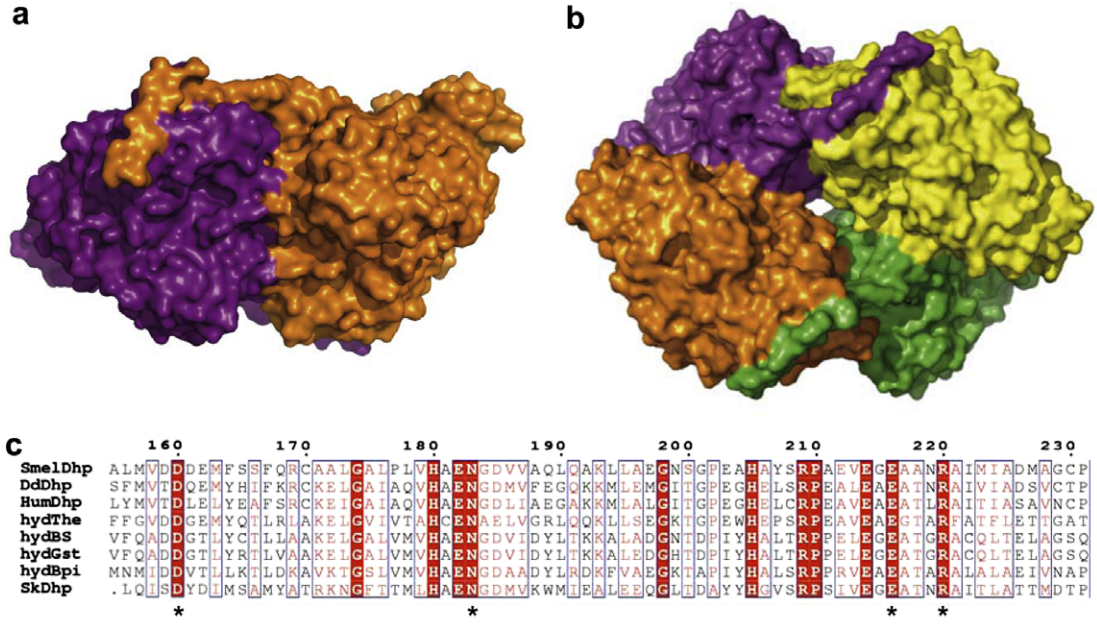

Fig. 2. (a) Dimeric and (b) tetrameric arrangement of SmelDhp showing the swap-like c-tail extensions. (c) Sequence alignment of SmelDhp with the other hydantoinases/dihydropyrimidinases whose structures are known to date, highlighting totally conserved residues in the dimerisation interface. DdDhp, dihydropyrimidinase from *Dictyostelium discoideum* (PDB ID. 2FTW); HumDhp, human collapsin response mediator protein 2 (PDB ID. 2GSE); hydThe, hydantoinase from *Thermus* sp. (PDB ID. 1GKP); hydBS, hydantoinase from *Bacillus stearothermophilus* (PDB ID. 1K1D); hydGst, hydantoinase from *Geobacillus stearothermophilus* (PDB ID. 1YNY); hydBpi, hydantoinase from *Burkholderia pickettii* (PDB ID. 1NFG); SkDhp, dihydropyrimidinase from *Saccharomyces kluyveri* (PDB ID. 2FTY).

the isolated dimer could not be detected under any experimental conditions.

3.4. C-terminus elongation, a possible evolutionary reminiscent for oligomerisation?

The c-termini of these enzymes vary greatly in length and similarity among enzymes from different organisms, as observed by Kim and Kim (1998). However, when focusing only on the α-proteobacterium kingdom, a Blast search with SmelDhp sequence shows that this c-tail is highly conserved in organisms such as *Pseudomonas*, *Agrobacterium* and *Ochrobactrum* genera (data not shown). Together with the swap domain-like manner in which the subunits are arranged, it shows that this c-terminus elongation might be involved in oligomerisation. A similar arrangement has been detected in the c-termini of cytosine deaminase, another member of the amidohydrolase family (Ireton et al., 2002). An arginine residue appears completely conserved for the dihydropyrimidinases/hydantoinases in α-proteobacterium kingdom (Arg476 for SmelDhp), which when mutated to alanine or deleted in the dimeric hydantoinase from *Pseudomonas putida* dissembled the enzyme to a monomeric form (Niu et al., 2007). SmelDhp Arg476 is responsible for five hydrogen bonds (per monomer) with Glu203, Asp274 and Tyr272, as well as several van der Walls interactions with other residues, and would support the relevance of the counterpart residue in the *Pseudomonas* enzyme. However, the mutation of SmelDhp Arg476 to alanine do not cause the dissociation of the tetramer (data not shown), and thus does not seems be crucial for oligomerisation in this enzyme. As one of the mechanisms proposed for the evolution of oligomeric interfaces is three-dimensional domain swapping (Bennett et al., 1995), we hypothesise that this c-tail might be a reminiscent evolutionary tactic used by nature to evolve the oligomeric state of these enzymes in this kingdom, facilitating evolution of the above-mentioned dimerisation interface. As SmelDhp is already at a further evolutionary oligomeric stage, tetramerisation interfaces might hamper dimer dissociation, as it occurs with *Pseudomonas* homologue (Niu et al., 2007).

3.5. The catalytic centre: structural resemblance to the amidohydrolase superfamily

Since Holm and Sander (1997) highlighted the homology among the amidohydrolase family, several enzymes have been identified as belonging in the same group. A DaliLite v.3 search (Holm et al., 2008) revealed several homologues for SmelDhp with a *Z*-score of over 10 (Table 4). SmelDhp shares with them a striking topology, with a common core formed by the catalityc $(\alpha/\beta)_8$ barrel, containing a binuclear centre at the end of the beta-strands of the barrel (H56, H58, Kcx147, H180, H236 and D313). Functionally equivalent residues involved in coordinating the metal ions are completely conserved in allantoinase, iso-aspartyl dipeptidase, adenine deaminase, urease, phosphotriesterase, aryldialkylphosphatases and dihydroorotase: they superimpose perfectly between structures (Table 4 and Fig. 3). It appears that this binuclear centre has been chosen by nature to accomplish several distinct hydrolytic reactions, even when a post-translational carboxylation of the ε-amino group of the lysine is necessary. *In vitro* experiments have proved that this kind of binuclear metal centre self-assembles in the presence of bicarbonate and the appropriate divalent cation (Shim and Raushel 2000). It therefore occurs spontaneously due to the atmospheric CO_2 which is dissolved in any solution. In the dihydropyrimidinase structures known to date, only that belonging to *Bacillus* sp. has been reported not to be carboxylated (Radha Kishan et al., 2005), although the deposited structure factors (PDB ID. 1YNY) show a clear positive electron density over a 5σ cut-off level, suggesting the presence of this modification.

A bridging water/hydroxide always appears between the metal ions in this kind of binuclear centre (wat925 and wat1042 for chains A and B in SmelDhp, respectively, Figs. 4 and 5). The metal ions play a crucial role in the polarization of the water molecule, allowing proton retrievement by a completely conserved Asp residue (see Table 4, Asp313 in SmelDhp), forming a nucleophilic hydroxyl group responsible for the hydrolysis of the amide bond of the substrates. Apart from this water molecule, a clear electron density appears next to the Zn atom which is further away from

Table 4
Several homologue enzymes of dihydropyrimidinases obtained using the Dalilite v.3 server. Although not all the enzymes present a bimetallic centre, counterpart residues appear in the table. NAG6PD: *N*-acetylglucosamine-6-phosphate deacetylase; NIAIA: *N*-isopropylammelide isopropyl amidohydrolase; αAβCεSD: α-amino-β-carboxymuconate-ε-semialdehyde decarboxylase.

Enzyme	PDB ID.	*Z*	% id.	RMSD (Å)	Composite domain	Metal 1		Bridge		Metal2	
SmelDhp	3DC8 (A)				Yes	H56	H58	Kcx147	D313	H180	H236
CRMP-2	2GSE (A)	60.7	45	1.2	Yes	–	–	–	–	–	–
CRMP-1	1KCX (B)	59.6	46	1.2	Yes	–	–	–	–	–	–
Allantoinase	3E74 (B)	48.2	27	2.0	Yes	H59	H61	Kcx146	D315	H186	H242
Dihydroorotase[b]	1XRF (A)	38.1	27	2.3	Yes	H61	H63	D153	D305	H180	H232
Dihydroorotase	1J79 (B)	31.8	15	2.6	No	H16	H18	Kcx102	D250	H139	H177
Iso-aspartyl dipeptidase	1PO9 (A)	28.6	17	2.8	Yes	H68	H70	Kcx162	D285	H201	H230
NAG6PD	1UN7 (B)	24.9	16	3.3	Yes	H63	H65	E136	D281	H202	H223
D-Aminoacylase	1M7J (A)	27.4	19	3.0	Yes	H67	H69	C96	D366	H220	H250
Enamidase	2VUN (D)	25.0	16	2.9	Yes	H67	H69	E164	D276	H193	H220
Adenine deaminase	2ICS (A)	24.7	15	3.3	Yes	H60	H62	Kcx154	D272	H188	H211
NIAIA[b]	2QT3 (A)	24.3	15	3.9	Yes	H60	H62		D303	H217	H249
Urease α-subunit	1FWC (C)	23.6	17	2.9	Yes	H134	H136	Kcx217	D360	H246	H272
Imidazolonepropionase[b]	2BB0 (B)	22.2	17	3.5	Yes	H80	H82		D324		H249
Cytosine deaminase[b]	1K6W (A)	20.7	16	4.3	Yes	H61	H63		D313	H214	H246
Phosphotriesterase	1PSC (B)	18.1	15	3.0	No[a]	H55	H57	Kcx169	D301	H201	H230
Aryldialkylphosphatase	2VC5 (A)	16.7	11	3.2	No[a]	H22	H24	Kcx137	D256	H170	H199
αAβCεSD[b]	2HBV (B)	16.5	14	3.1	No	H9	H11		D294	H177	H228
Renal dipeptidase	1ITQ (A)	14.5	11	3.4	No	H20	D22	E125	D288	H198	H219

[a]It presents two β-sheets in the N-termini.
[b]The structure corresponding to these enzymes only presented one metal bound, and those residues proposed in metal binding are highlighted.

the proton shuffling Asp313 (Zn-β). We have attributed a water molecule to this density (wat620 for chain A and wat1041 for chain B, Fig. 5), although it could also be due to the presence in the crystallisation solution of a formate or acetate ion, whose carbonyl group resembles the carbonyl group (C4) of the substrate, due to some extra density in chain A (assigned as wat1037). Furthermore, it is at binding distance of Tyr152 (Fig. 5). Although this second metal-coordinated water molecule has not been reported in all the hydantoinase structures known, its analogy with other amidohydrolases supports the first step of the hydrolysis mechanism proposed previously (Lohkamp et al., 2006). In this proposed mechanism a water molecule in the coordination sphere of the Zn-β is said to be replaced by the oxo group of the incoming substrate (Fig. 4).

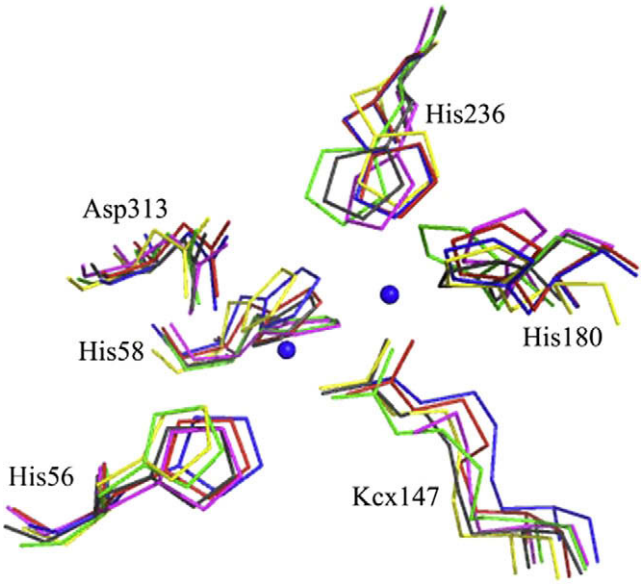

Fig. 3. Superposition of the bimetallic centre of several members of the amidohydrolase superfamily. SmelDhp, including Zn ions (PDB ID. 3DC8, blue), allantoinase (PDB ID. 3E74, red), iso-aspartyl dipeptidase (PDB ID. 1PO9, green), adenine deaminase (PDB ID. 2ICS, yellow), urease (PDB ID. 1FWC, magenta) and phosphotriesterase (PDB ID. 1PSC, dark grey). (For interpretation of the references to color in this figure legend, the reader is referred to the web version of this paper.)

3.6. Accommodation of the substrate in the binding pocket

The tetrameric molecular arrangement of SmelDhp leaves the end of the barrels (where the catalytic centre is located) facing toward the solvent, allowing SmelDhp to sequester its substrate efficiently. In this cleft, three non-conserved loops, comprising L59–D70, A91–S98 and M150–V158 close the cavity where the substrate would enter. These loops were previously reported as Stereo Gate Loops (SGLs), and described as being responsible for controlling the substrate specificity of D-hydantoinases (Cheon et al., 2002). The corresponding loops are known to appear in other amidohydrolases covering the entrance of the catalytic cleft, and in some cases they flap upon substrate binding (Liaw et al., 2003, and references cited therein). Although the highest temperature factors in SmelDhp structure were found in the loops at the entrance of the catalytic cleft, there is no experimental evidence to support this hypothesis in dihydropyrimidinases.

By analogy with the dihydropyrimidinase from *Saccharomyces kluyveri* (^{Sk}DHPase), the SmelDhp residues involved in substrate binding are Asn334 and Ser286 (Supplementary Figure S3) (the latter being spatially conserved in other enzymes from the amidohydrolase family such as allantoinase (PDB ID. 3E74, Ser288), imidazolonepropionase (PDB 2BB0, Ser329) and D-aminoacylase (PDB ID. 1M7J, Ser289). In the second SGL described above, a completely conserved Tyrosine (Tyr152 in SmelDhp) appears, for which an important role in stabilization of a tetrahedral transition state was already suggested by Lohkamp et al. (2006). However, controversy regarding the significance of this residue in substrate binding/hydrolysis arises from mutational studies (Cheon et al., 2003) and structural analysis (Lohkamp et al., 2006). The structure of ^{Sk}DHPase shows that the corresponding residue (Tyr172) is not at binding distance from the substrate dihydrouracil (PDB ID. 2FVK, Supplementary Figure S3), most probably due to the absence of clear electron densities for this residue, though it is at binding distance from the amine group of the reaction product (PDB ID. 2FVM). On the other hand, mutation of the counterpart tyrosine in *Bacillus stearothermophilus* D1 enzyme (Tyr155, Cheon et al., 2003) and that from SmelDhp, results in inactivation of the

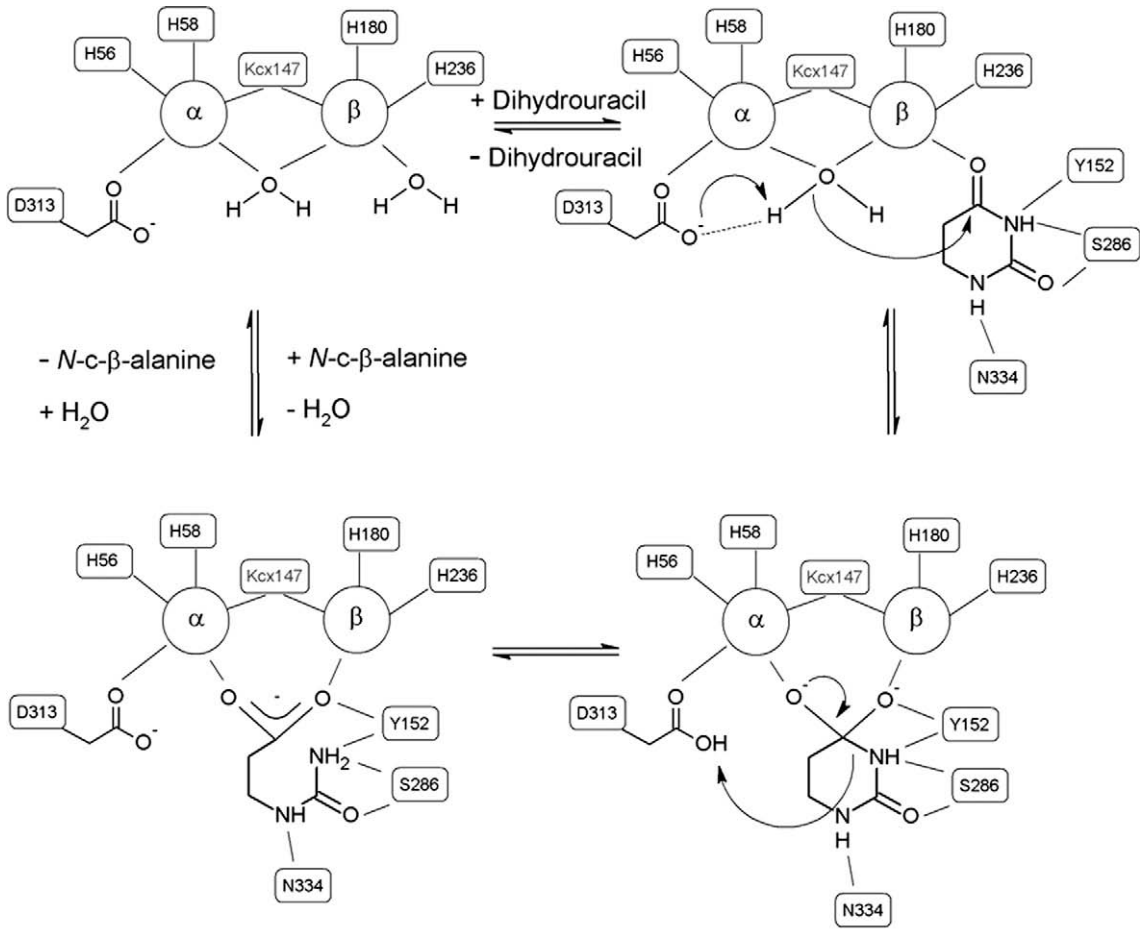

Fig. 4. Proposed reaction mechanism of SmelDhp based on structural and kinetic features, and on those previously proposed by Thoden et al. (2001) and Lohkamp et al. (2006).

enzymes. Circular dichroism and Gel filtration experiments with SmelDhp Y152A mutant suggest that these results do not arise from a change in the secondary or quaternary structure of SmelDhp (data not shown), thus supporting a direct relationship of this residue in enzymatic activity. As this tyrosine is at binding distance of the replaced water molecule in the Zn-β environment, the evidences suggest that this residue might support correct positioning of the substrate, and also polarise the scissile amide bond together with Zn-β, facilitating the attack of an activated hydroxyl group (from the abstraction of a proton of the binuclear metal centre bridging water polarized by Zn-α, carried out by Asp313). However, more results are needed to asseverate a key role of this tyrosine not only in product stabilization but also in substrate binding.

3.7. Structural relationship with substrate specificity

When analysing only the five-membered ring substrates, it is clear that the presence of the substitutent in the carbon 5 of the hydantoin favours the binding of the substrate (Table 3). Manual modelling of the substrate shows that the L-conformation of the substrate would cause steric hindrance with the Zn-β of the enzyme, while the lateral chain for a D-substituted hydantoin can fit in the "hydrophobic pocket" conformed by the SGLs described above (data not shown). The turn-over number and the catalytic efficiency (k_{cat}/K_m) for the non-ramified aliphatic 5-monosubstituted hydantoins show an increasing value for the shorter chain (D-MH > D-EH > D-PROPH > D-BUTH). However, the affinity for those substrates does not follow the same tendency, and seems to be favoured for the longer chains, suggesting that a bulkier apolar substituent favours the binding (Table 3). Due to solubility problems of the studied 6-monosubstitued dihydrouracils, only the K_m for three substrates could be obtained. Comparing the affinity of the enzyme for the 5- and 6-methyl-dihydrouracil, it is clear that the substitution in carbon 6 of dihydrouracil produces some interaction/clash in the catalytic centre of the enzyme decreasing its affinity by two orders of magnitude (Table 3). Manual docking of dihydrouracil in the catalytic centre of SmelDhp suggests clashes of the lateral chain of 6-monosubustituted dihydrouracils with His58, Met61, Phe63 and/or Cys315. This could explain the lower activity detected with bulky lateral chains such as phenyl or isobutyl.

Here we present the first experimental evidence of a dihydropyrimidinase that is active toward non-natural monosubstituted dihydrouracils. Recently, we have characterised an *N*-carbamoyl-β-amino acid amidohydrolase from *Agrobacterium tumefaciens* able to hydrolyse several non-natural *N*-carbamoyl-β-amino acids (Martínez-Gómez et al., 2009). Although further experiments must be carried out, preliminary results have shown that both enzymes can be coupled to obtain potentially different β-amino acids from monosubstituted dihydrouracils, which in the future might be useful for the enzymatic production of these compounds.

Furthermore, we establish some new insights into the structure of this kind of enzyme, which might shed some light on our knowledge of the amidohydrolase family. The c-terminal domain common in the α-proteobacterium kingdom forms a swap-like domain, which by comparison with the data available for the

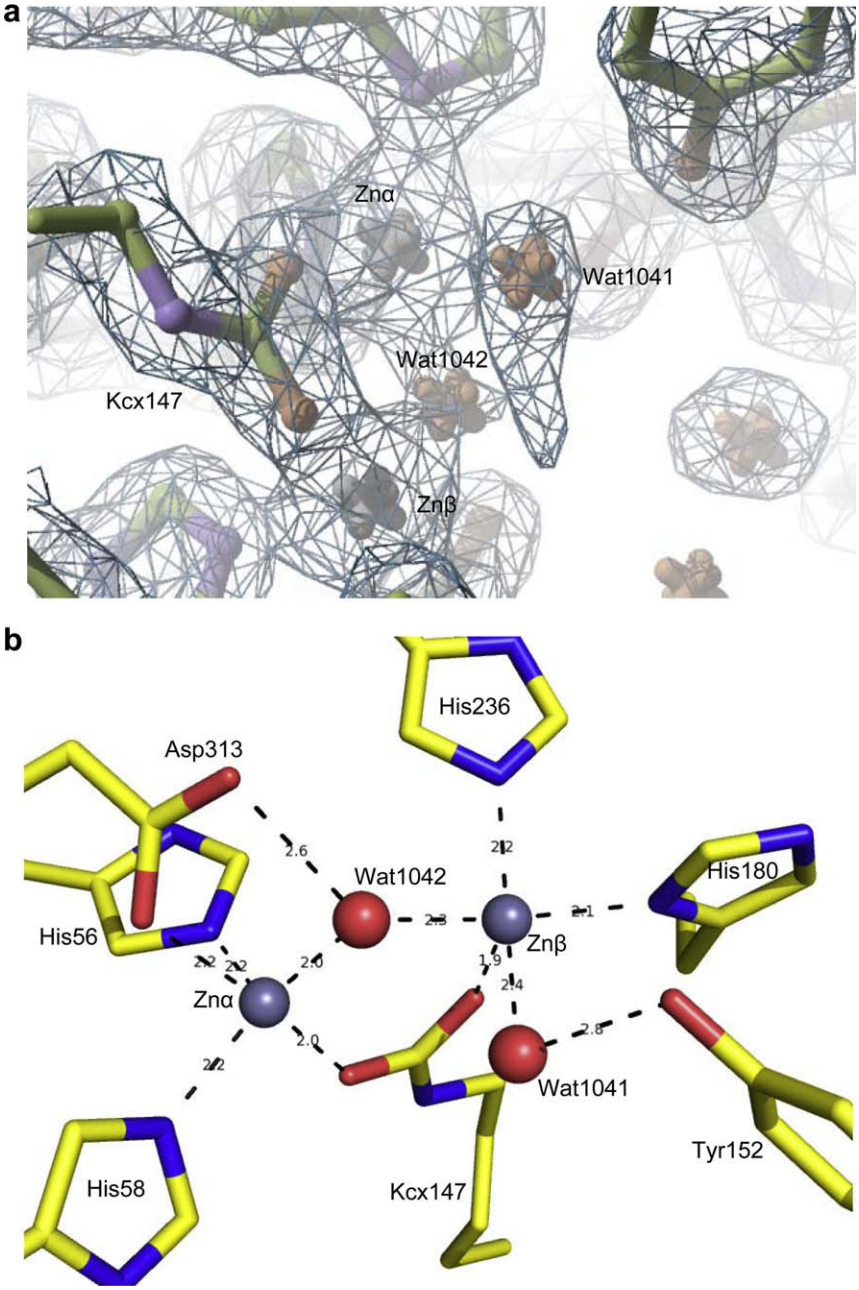

Fig. 5. (a) $2F_o - F_c$ map at 1.6σ contours, including the binuclear Zn-centre (from chain B) and the two water molecules at binding distance from the metal cations. (b) Coordination geometry for the binuclear metal centre of SmelDhp, showing the atomic distances.

Pseudomonas enzyme, suggests an evolutionary tactic for dimerisation of dihydropyrimidinase in this kingdom, which seems not to be necessary for tetramerisation. Highly conserved residues in the dimerisation surface of dihydropyrimidinases (Fig. 2C) suggest a key role in protein assembly, although further investigation is being carried out to support this fact. The importance of a conserved tyrosine is highlighted, allowing us to infer a slightly different reaction mechanism to that previously proposed for these enzymes.

Acknowledgments

This work was supported by the Spanish Ministry of Education and Science BIO2007-67009 and Andalusian Regional Council of Innovation, Science and Technology CV7-02651 projects, COST Action CM0701 and OptiCryst project of the Sixth Frame Work, UE. SMR was supported by the Andalusian Regional Government, Spain. The authors thank Andy Taylor for critical discussion of the manuscript and Pedro Madrid-Romero for technical assistance. This is a product of the "Factoría Española de Cristalización", Consolider-Ingenio 2010 project (MEC).

Appendix A. Supplementary data

Supplementary data associated with this article can be found, in the online version, at doi:10.1016/j.jsb.2009.10.013.

References

Abendroth, J., Niefind, K., May, O., Siemann, M., Syldatk, C., Schomburg, D., 2002a. The structure of D-hydantoinase from *Arthobacter aurescens* leads to an understanding of dihydropyrimidinase substrate and enantio specificity. Biochemistry 41, 8589–8597.

Abendroth, J., Niefind, K., Schomburg, D., 2002b. X-ray structure of a dihydropyrimidinase from *Thermus* sp. at 1.3 Å resolution. J. Mol. Biol. 320, 143–156.

Bennett, M.J., Schlunegger, M.P., Eisenberg, D., 1995. 3D domain swapping: a mechanism for oligomer assembly. Protein Sci. 4, 2455–2468.

Cheon, Y.-H., Kim, H.-S., Han, K.-H., Abendroth, J., Niefind, K., Schomburg, D., Wang, J., Kim, Y., 2002. Crystal structure of D-hydantoinase from *Bacillus stearothermophilus*: insight into the stereochemistry of enantioselectivity. Biochemistry 41, 9410–9417.

Cheon, Y.-H., Park, H.-S., Lee, S.-C., Lee, D.-E., Kim, H.-S., 2003. Structure-based mutational analysis of the active site residues of D-hydantoinase. J. Mol. Catal. B 26, 217–222.

Clemente-Jiménez, J.M., Martínez-Rodríguez, S., Rodríguez-Vico, F., Las Heras-Vázquez, F.J., 2008. Optically pure α-amino acids production by the "Hydantoinase Process". Recent Patents Biotechnol. 2, 35–46.

DeLano, W.L., 2002 The PyMOL Molecular Graphics System on World Wide Web. Available from: <http://www.pymol.org>.

Deo, R.C., Schmidt, E.F., Elhabazi, A., Togashi, H., Burley, S.K., Strittmatter, S.M., 2004. Structural bases for CRMP function in plexin-dependent semaphorin3A signaling. EMBO J. 23, 9–22.

Emsley, P., Cowtan, K., 2004. Coot: model-building tools for molecular graphics. Acta Crystallogr. Sect. D 60, 2126–2132.

Holm, L., Sander, C., 1997. An evolutionary treasure: unification of a broad set of amidohydrolases related to urease. Proteins 28, 72–82.

Holm, L., Kaariainen, S., Rosenstrom, P., Schenkel, A., 2008. Searching protein structure databases with DaliLite v.3. Bioinformatics 24, 2780–2781.

Hooft, R.W.W., Vriend, G., Sander, C., Abola, E.E., 1996. Errors in protein structures. Nature 381, 272.

Ireton, G.C., McDermott, G., Black, M.E., Stoddard, B.L., 2002. The structure of *Escherichia coli* cytosine deaminase. J. Mol. Biol. 315, 687–697.

Jozic, D., Kaiser, J.T., Huber, R., Bode, W., Maskos, K., 2003. X-ray structure of isoaspartyl dipeptidase from *E. coli*: a dinuclear zinc peptidase evolved from amidohydrolases. J. Mol. Biol. 332, 243–256.

Kim, G.-J., Kim, H.-S., 1998. C-terminal regions of D-hydantoinases are nonessential for catalysis, but affect the oligomeric structure. Biochem. Biophys. Res. Commun. 243, 96–100.

Kim, K., Kim, M.I., Chung, J., Ahn, J.H., Rhee, S., 2009. Crystal structure of metal-dependent allantoinase from *Escherichia coli*. J. Mol. Biol. 387, 1067–1074.

Kress, D., Alhapel, A., Pierik, A.J., Essen, L.O., 2008. The crystal structure of enamidase: a bifunctional enzyme of the nicotinate catabolism. J. Mol. Biol. 384, 837–847.

Krissinel, E., Henrick, K., 2007. Inference of macromolecular assemblies from crystalline state. J. Mol. Biol. 372, 774–797.

Las Heras-Vázquez, F.J., Martínez-Rodríguez, S., Mingorance-Cazorla, L., Clemente-Jiménez, J.M., Rodríguez-Vico, F., 2003. Overexpression and characterization of hydantoin racemase from *Agrobacterium tumefaciens* C58. Biochem. Biophys. Res. Commun. 303, 541–547.

Laskowski, R.A., Moss, D.S., Thornton, J.M., 1993. Main-chain bond lengths and bond angles in protein structures. J. Mol. Biol. 231, 1049–1067.

Laskowski, R.A., Chistyakov, V.V., Thornton, J.M., 2005. PDBsum more: new summaries and analyses of the known 3D structures of proteins and nucleic acids. Nucleic Acids Res. 33, D266–D268.

Lee, S.-G., Lee, D.-C., Hong, S.-P., Sung, M.-H., Kim, H.-S., 1995. Thermostable D-hydantoinase from thermophilic *Bacillus stearothermophilus* SD-1: characteristics of purified enzyme. Appl. Microbiol. Biotechnol. 43, 270–276.

Liaw, S.H., Chen, S.J., Ko, T.P., Hsu, C.S., Chen, C.J., Wang, A.H., Tsai, Y.C., 2003. Crystal structure of D-aminoacylase from *Alcaligenes faecalis* DA1. A novel subset of amidohydrolases and insights into the enzyme mechanism. J. Biol. Chem. 278, 4957–4962.

Lohkamp, B., Andersen, B., Piskur, J., Dobritzsch, D., 2006. The crystal structures of dihydropyrimidinases reaffirm the close relationship between cyclic amidohydrolases and explain their substrate specificity. J. Biol. Chem. 281, 13762–13776.

Lovell, S.C., Davis, I.W., Arendall 3rd, W.B., de Bakker, P.I., Word, J.M., Prisant, M.G., Richardson, J.S., Richardson, D.C., 2003. Structure validation by Calpha geometry: phi,psi and Cbeta deviation. Proteins 50, 437–450.

Martin, P.D., Purcarea, C., Zhang, P., Vaishnav, A., Sadecki, S., Guy-Evans, H.I., Evans, D.R., Edwards, B.F., 2005. The crystal structure of a novel, latent dihydroorotase from *Aquifex aeolicus* at 1.7 Å resolution. J. Mol. Biol. 348, 535–547.

Martínez-Gómez, A.I., Martínez-Rodríguez, S., Clemente-Jiménez, J.M., Pozo-Dengra, J., Rodríguez-Vico, F., Las Heras-Vázquez, F.J., 2007. Recombinant polycistronic structure of hydantoinase process genes in *Escherichia coli* for the production of optically pure D-amino acids. Appl. Environ. Microbiol. 73, 1525–1531.

Martínez-Gómez, A.I., Martínez-Rodríguez, S., Pozo-Dengra, J., Tessaro, D., Servi, S., Clemente-Jiménez, J.M., Rodríguez-Vico, F., Las Heras-Vázquez, F.J., 2009. Potential application of *N*-carbamoyl-β-alanine amidohydrolase from *Agrobacterium tumefaciens* C58 for β-amino acid production. Appl. Environ. Microbiol. 75, 514–520.

Martínez-Rodríguez, S., Las Heras-Vázquez, F.J., Clemente-Jiménez, J.M., Mingorance-Cazorla, L., Rodríguez-Vico, F., 2002. Complete conversion of D,L-5-monosubstituted hydantoins with a low velocity of chemical racemization into D-amino acids using whole cells of recombinant *Escherichia coli*. Biotechnol. Prog. 18, 1201–1206.

Martínez-Rodríguez, S., Las Heras-Vázquez, F.J., Clemente-Jiménez, J.M., Rodríguez-Vico, F., 2004a. Biochemical characterization of a novel hydantoin racemase from *Agrobacterium tumefaciens* C58. Biochimie 86, 77–81.

Martínez-Rodríguez, S., Las Heras-Vázquez, F.J., Mingorance-Cazorla, L., Clemente-Jiménez, J.M., Rodríguez-Vico, F., 2004b. Molecular cloning, purification, and biochemical characterization of hydantoin racemase from the legume symbiont *Sinorhizobium meliloti* CECT 4114. Appl. Environ. Microbiol. 70, 625–630.

Martínez-Rodríguez, S., González-Ramírez, L.A., Clemente-Jiménez, J.M., Rodríguez-Vico, F., Las Heras-Vázquez, F.J., Gavira, J.A., García-Ruíz, J.M., 2006. Crystallisation and preliminary crystallographic studies of the recombinant dihydropyrimidinase from *Sinorhizobium meliloti* CECT4114. Acta Crystallogr. Sect. F 62, 1223–1226.

Martínez-Rodríguez, S., Clemente-Jiménez, J.M., Rodríguez-Vico, F., Las Heras-Vázquez, F.J., 2007. D-Amino acids: a new frontier in amino acid and protein research, Konno et al. R. (Eds.), Nova Science Inc., New York, pp. 573–577.

Martínez-Rodríguez, S., Encinar, J.A., Hurtado-Gómez, E., Prieto, J., Clemente-Jiménez, J.M., Las Heras-Vázquez, F.J., Rodríguez-Vico, F., Neira, J.L., 2009. Metal-triggered changes in the stability and secondary structure of a tetrameric dihydropyrimidinase: a biophysical characterization. Biophys. Chem. 139, 42–52.

Murshudov, G.N., Vagin, A.A., Dodson, E.J., 1997. Refinement of macromolecular structures by the maximum-likelihood method. Acta Crystallogr. Sect. D 53, 240–255.

Niu, L., Zhang, X., Shi, Y., Yuan, J., 2007. Subunit dissociation and stability alteration of D-hydantoinase deleted at the terminal amino acid residue. Biotechnol. Lett. 29, 303–308.

Radha Kishan, K.V., Vohra, R.M., Ganesan, K., Agrawal, V., Sharma, V.M., Sharma, R., 2005. Molecular structure of D-hydantoinase from *Bacillus* sp. AR9: evidence for mercury inhibition. J. Mol. Biol. 347, 95–105.

Schwede, T., Diemand, A., Guex, N., Peitsch, M.C., 2000. Protein structure computing in the genomic era. Res. Microbiol. 151, 107–112.

Seibert, C.M., Raushel, F.M., 2005. Structural and catalytic diversity within the amidohydrolase superfamily. Biochemistry 44, 6383–6391.

Shim, H., Raushel, F.M., 2000. Self-assembly of the binuclear metal center of phosphotriesterase. Biochemistry 39, 7357–7364.

Sumi, S., Imaeda, M., Kidouchi, K., Ohba, S., Hamajima, N., Kodama, K., Togari, H., Wada, Y., 1998. Population and family studies of dihydropyrimidinuria: prevalence, inheritance mode, and risk of fluorouracil toxicity. Am. J. Med. Genet. 78, 336–340.

Thoden, J.B., Phillips Jr., G.N., Neal, T.M., Raushel, F.M., Holden, H.M., 2001. Molecular structure of dihydroorotase: a paradigm for catalysis through the use of a binuclear metal center. Biochemistry 40, 6989–6997.

van Kuilenburg, A.B.P., 2004. Dihydropyrimidine dehydrogenase and the efficacy and toxicity of 5-fluorouracil. Eur. J. Cancer 40, 939–950.

van Kuilenburg, A.B.P., Meinsma, J.R., Zonnenberg, B.A., Zoetekouw, L., Baas, F., Matsuda, K., Tamaki, N., van Gennip, A.H., 2003. Dihydropyrimidinase deficiency and severe 5-fluorouracil toxicity. Clin. Cancer Res. 9, 4363–4367.

van Kuilenburg, A.B., Meijer, J., Dobritzsch, D., Meinsma, R., Duran, M., Lohkamp, B., Zoetekouw, L., Abeling, N.G., van Tinteren, H.L., Bosch, A.M., 2007. Clinical, biochemical and genetic findings in two siblings with a dihydropyrimidinase deficiency. Mol. Genet. Metab. 91, 157–164.

Vincent, F., Yates, D., Garman, E., Davies, G.J., Brannigan, J.A., 2004. The three-dimensional structure of the *N*-acetylglucosamine-6-phosphate deacetylase, NagA, from *Bacillus subtilis*: a member of the urease superfamily. J. Biol. Chem. 279, 2809–2816.

Ware, E., 1950. The chemistry of the hydantoins. Chem. Rev. 46, 403–470.

Winn, M.D., Isupov, M.N., Murshudov, G.N., 2001. Use of TLS parameters to model anisotropic displacements in macromolecular refinement. Acta Crystallogr. Sect. D 57, 122–133.

Xu, G., West, T.P., 1994. Characterization of dihydropyrimidinase from *Pseudomonas stutzeri*. Arch. Microbiol. 161, 70–74.

Xu, Z., Liu, Y., Yang, Y., Jiang, W., Arnold, E., Ding, J., 2003. Crystal structure of D-hydantoinase from *Burkholderia pickettii* at a resolution of 2.7 Å: insights into the molecular basis of enzyme thermostability. J. Bacteriol. 185, 4038–4049.

Yu, Y., Liang, Y.H., Brostromer, E., Quan, J.M., Panjikar, S., Dong, Y.H., Su, X.D., 2006. A catalytic mechanism revealed by the crystal structures of the imidazolonepropionase from *Bacillus subtilis*. J. Biol. Chem. 281, 36929–36936.